JACS
JOURNAL OF THE AMERICAN CHEMICAL SOCIETY

ARTICLE

pubs.acs.org/JACS

Hydrogen Exchange Mass Spectrometry of Bacteriorhodopsin Reveals Light-Induced Changes in the Structural Dynamics of a Biomolecular Machine

Yan Pan,[†] Leonid Brown,[‡] and Lars Konermann*[,†]

[†]Department of Chemistry, The University of Western Ontario, London, Ontario, Canada N6A 5B7

[‡]Department of Physics, University of Guelph, Guelph, Ontario, Canada N1G 2W1

Supporting Information

ABSTRACT: Many proteins act as molecular machines that are fuelled by a nonthermal energy source. Examples include transmembrane pumps and stator−rotor complexes. These systems undergo cyclic motions (CMs) that are being driven along a well-defined conformational trajectory. Superimposed on these CMs are thermal fluctuations (TFs) that are coupled to stochastic motions of the solvent. Here we explore whether the TFs of a molecular machine are affected by the occurrence of CMs. Bacteriorhodopsin (BR) is a light-driven proton pump that serves as a model system in this study. The function of BR is based on a photocycle that involves trans/cis isomerization of a retinal chromophore, as well as motions of transmembrane helices. Hydrogen/deuterium exchange (HDX) mass spectrometry was used to monitor the TFs of BR, focusing on the monomeric form of the protein. Comparative HDX studies were conducted under illumination and in the dark. The HDX kinetics of BR are dramatically accelerated in the presence of light. The isotope exchange rates and the number of backbone amides involved in EX2 opening transitions increase roughly 2-fold upon illumination. In contrast, light/dark control experiments on retinal-free protein produced no discernible differences. It can be concluded that the extent of TFs in BR strongly depends on photon-driven CMs. The light-induced differences in HDX behavior are ascribed to protein destabilization. Specifically, the thermodynamic stability of the dark-adapted protein is estimated to be 5.5 kJ mol^{-1} under the conditions of our work. This value represents the free energy difference between the folded state *F* and a significantly unfolded conformer *U*. Illumination reduces the stability of *F* by 2.2 kJ mol^{-1}. Mechanical agitation caused by isomerization of the chromophore is transferred to the surrounding protein scaffold, and subsequently, the energy dissipates into the solvent. Light-induced retinal motions therefore act analogously to an internal heat source that promotes the occurrence of TFs. Overall, our data highlight the potential of HDX methods for probing the structural dynamics of molecular machines under "engine on" and "engine off" conditions.

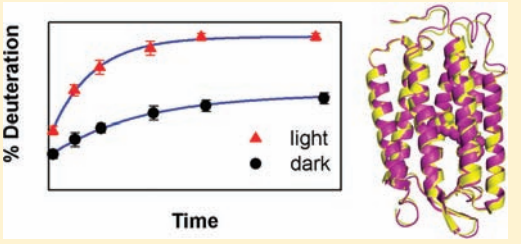

INTRODUCTION

Native proteins adopt unique structures that are linked to specific biological functions. However, these structures are not static. Numerous investigations have highlighted a close association between protein function and dynamics,[1−7] although the exact nature of this relationship remains a matter of debate.[8−11] Also, the term "conformational dynamics" can carry different connotations.[12] We propose the following classification:

(i) A *switching motion* (*SM*) represents an externally triggered conformational change. SMs are singular events that may be caused by ligand binding, covalent modifications, or an alteration in solvent environment. As a result of one of these factors, the conformational equilibrium of the protein shifts from one region of the energy landscape to another.[13]

(ii) Many proteins act as molecular machines that undergo externally driven *cyclic motions* (*CMs*). In contrast to thermal fluctuations (see below), CMs require a nonthermal energy source that drives structural changes along a well-defined cyclic trajectory. For example, a number of transporters in the cell membrane exploit energy stored in an ion concentration gradient to translocate substrate molecules across lipid bilayers. This pumping action involves protein motions that expose a substrate binding site alternatively to the cytoplasmic and the extracellular surface.[14−16] In a related fashion, the CMs of stator−rotor assemblies are energized by a proton-motive force or by nucleotide-triphosphate hydrolysis.[17,18] The salient feature that distinguishes SMs from CMs is the inherently repetitive nature of the latter.

(iii) All proteins undergo incessant *thermal fluctuations* (*TFs*) that are coupled to random motions of the surrounding solvent.[19] TFs are stochastic events that span a multitude of time and length scales, from picosecond movements of individual side chains to infrequent unfolding/refolding transitions of the entire protein.[12,20] At equilibrium, all

Received: July 4, 2011
Published: November 01, 2011

states on the energy landscape are populated according to their Boltzmann weights.[21] TFs lead to an ongoing interconversion between these states, with rates that are governed by free energy barriers.[12,20,22] SMs and CMs will generally be superimposed by TFs.

In many cases, the character of TFs is profoundly different before and after a SM has occurred. This relationship allows changes in protein switching state to be monitored by techniques that probe TFs.[23,24] In contrast, much less is known about the relationship between TFs and CMs.[25,26] One possibility is that TFs are more pronounced when a protein undergoes CMs. On the other hand, CMs often manifest themselves as rigid-body movements,[27,28] and it seems conceivable that these motions might have only minor effects on TFs. The current work explores this issue by monitoring the dynamics of a molecular machine under "engine-on" and "engine-off" conditions.

TFs can be probed by a variety of techniques. These include computer simulations,[29] crystallographic temperature factors,[12] single molecule fluorescence assays,[30] quasielastic neutron scattering,[26] Mössbauer spectroscopy,[20] and NMR spin relaxation measurements.[31] In addition, amide hydrogen/deuterium exchange (HDX) methods are being widely used. The readout of HDX experiments may be performed by NMR,[32] infrared spectroscopy,[6] and mass spectrometry (MS).[33−36] The latter approach is particularly attractive due to its conceptual simplicity, high sensitivity, the possibility to distinguish coexisting protein conformers, and the capability to study proteins that are beyond the NMR size range.

In typical continuous-labeling HDX experiments, the protein is placed in a D_2O-containing environment, and deuterium incorporation is monitored as a function of time.[32] Backbone amide hydrogens can reside either in a closed or in an open state.[37] Closed sites are protected from exchange, either by N—H····O=C hydrogen bonding or by solvent exclusion (or a combination of both). Open sites are not involved in hydrogen bonding, and they are accessible to the solvent.[38] HDX at these unprotected sites proceeds with a chemical rate constant k_{ch}.[39] Most amide groups in natively folded proteins predominantly reside in a closed state. Slow HDX at these sites nonetheless takes place due to short-lived excursions to open conformations. As a result of these TFs, each amide group undergoes exchange with a characteristic rate constant k_{HDX}. Opening and closing rate constants are designated as k_{op} and k_{cl}, respectively, and the overall HDX mechanism can be described as[32,40]

$$H_{closed} \underset{k_{cl}}{\overset{k_{op}}{\rightleftharpoons}} H_{open} \xrightarrow[D_2O]{k_{ch}} \text{exchanged} \quad (1)$$

The EX1 regime ($k_{ch} \gg k_{cl}$) is characterized by $k_{HDX} = k_{op}$. Under EX2 conditions ($k_{cl} \gg k_{ch}$), isotope exchange occurs with $k_{HDX} = K_{op} \times k_{ch}$, where $K_{op} = (k_{op}/k_{cl})$. The free energy difference associated with opening of an amide group in the EX2 regime is

$$\Delta G^{EX2} = -RT \ln K_{op} \quad (2)$$

Most HDX investigations in the literature have focused on the effects of SMs.[23,34,41−47] Comparing "before" and "after" scenarios (such as free vs ligand-bound), those studies exploit the fact that the stability of a protein depends on its switching state, leading to differences in the TFs that modulate the EX2 kinetics according to eq 2.[48] In contrast to the numerous HDX studies devoted to SMs, there appear to be no prior attempts to explore whether the HDX behavior of molecular machines is sensitive to the occurrence of CMs.

Bacteriorhodopsin (BR) is a molecular machine that acts as a light-driven proton pump. In its natural purple membrane environment, BR is packed as trimers that form a two-dimensional lattice. However, monomers represent the functional unit of the protein.[49,50] Each monomer consists of seven transmembrane helices that are connected by short loops. In addition, the protein contains a central retinal chromophore that is bound to K216 via a Schiff base. H^+ translocation is mediated by a photocycle that starts with the light-adapted *all-trans*/15-*anti* ground state and proceeds through a number of sequential intermediates.[51−54] Photoisomerization of the retinal to the 13-*cis*/15-*anti* configuration represents the primary event. The resulting strained chromophore configuration drives all subsequent steps of the cycle.[54] Vectorial H^+ translocation involves proton transfer from the Schiff base to D85 and subsequent Schiff base reprotonation by D96. Reisomerization ultimately regenerates the BR ground state. The photocycle is coupled to various protein conformational changes[55,56] that involve partial rotation, tilting, and bending motions of helices.[57−60] In the dark, the retinal equilibrates between the *all-trans*/15-*anti* and 13-*cis*/15-*syn* forms.[61] Protein structural differences between the light-adapted ground state and dark-adapted BR are small when compared to the substantial motions that occur during the photocycle.[62]

BR represents a highly suitable test system for exploring a possible relationship between CMs and TFs. Under continuous illumination, the protein performs an ongoing cycle of structural transitions,[57,58] whereas many of these motions are absent in the dark.[62] We probe the extent of TFs in comparative HDX measurements with and without illumination. Under properly controlled conditions, our investigations reveal dramatically different isotope exchange kinetics that reflect a light-induced destabilization of the protein. It appears that this destabilization is caused by retinal-mediated mechanical agitation, which acts in a manner comparable to an internal heat source. Our findings highlight the utility of HDX techniques for studying the behavior of molecular machines.

METHODS

Proteins and Reagents. Purple membranes from *Halobacterium salinarum* were harvested and purified by sucrose gradient centrifugation as described previously,[63−65] resulting in aqueous stock suspensions with a BR concentration of 180 μM. Sodium dodecyl sulfate (SDS), sodium phosphate, and formic acid were from Sigma (St. Louis, MO). L-α-1,2-Dimyristoylphosphatidylcholine (DMPC) was obtained from Avanti (Alabaster, AL), and 3-[(3-cholamidopropyl)dimethylammonio]-1-propanesulfonate (CHAPS) was from Calbiochem (San Diego, CA). All chemicals were used as received.

Most experiments were conducted on monomeric BR[50,66] that was generated by refolding of SDS-denatured bacterioopsin (BO, the retinal-free form of the protein). SDS-denatured BO was prepared by delipidation as described,[67] and the absence of retinal was confirmed by UV−vis spectroscopy. Monomeric BR[50,66] was prepared by mixing SDS-denatured BO with *all-trans* retinal from an ethanol stock solution in equimolar retinal/protein ratio. Subsequently, 10 mM phosphate refolding buffer (pH 6) containing 2% DMPC/CHAPS bicelles was added to the mixture.[67] The regeneration yield of this procedure is on the order of 90%,[68] as confirmed on the basis of BR/BO peak intensity ratios in the mass spectra.[69] Monomeric BO was generated following the same procedure, but without addition of retinal. All samples were equilibrated overnight at room temperature in the dark. The resulting solutions contained 10 μM protein, 1% DMPC, 1% CHAPS, 0.1% SDS, and less than 0.2% (v/v) ethanol. The protein was concentrated 10-fold by lyophylization and subsequent resuspension in phosphate buffer. In

addition to studies on monomeric BR, we also conducted HDX measurements on intact purple membranes. For these measurements, purple membrane stock suspension was diluted with phosphate buffer to a protein concentration of 100 μM. The final buffer concentration was 100 mM. All other steps were performed as described below for the monomeric samples.

Hydrogen/Deuterium Exchange under Light/Dark Conditions. All HDX experiments of this work were conducted in continuous-labeling mode. In order to promote extensive isotope exchange, HDX was conducted in mildly basic solution (pH meter reading 8.5). Chemical exchange rate constants k_{ch} under these conditions are in the range of 1000 s^{-1}, roughly 3 orders of magnitude higher than in neutral solution.[39,70] This difference in pH is the reason for the greater exchange levels observed in the current work, as compared to previous experiments that were conducted at a pH meter reading of 6.[69] BR consists of 248 residues, 11 of which are prolines, such that the number of backbone N−H groups is 236.[69] Isotope labeling was initiated by mixing the protein solutions with D_2O-based buffer (100 mM sodium phosphate) in a 1:4 volume ratio. The resulting solution was transferred into two identical microcentrifuge tubes (Eppendorf, Hamburg, Germany) that had their lids fitted with transparent windows made from glass coverslips fastened with epoxy glue. Each tube contained 350 μL of protein solution. One tube was wrapped in aluminum foil and kept in the dark. The other one was continuously illuminated at 530 nm using a Thorlabs light-emitting diode (model M530L1, Newton, NJ) that was operated using a 275 mW power supply. The light source was fitted with a collimator, and the protein samples were irradiated from above through the transparent lid with a distance of 3 cm between the collimator output and the surface of the solution. Both tubes were thermostatted at 26 °C in a circulating water bath; a digital resistance thermometer was used to confirm that light and dark samples were at the same temperature. 35 μL aliquots were removed at various time points, ranging from 4 min to 48 h. These aliquots were quenched by mixing with 3 μL of 2 M hydrochloric acid for a final pH of 2.4, followed by flash freezing in liquid nitrogen.

Liquid Chromatography/Mass Spectrometry. LC/MS measurements were conducted under conditions that preserve retinal binding to BR,[69] such that the HDX properties of BR and BO subpopulations in bulk solution could be tracked independently. The analyses were performed using a Waters Acquity UPLC instrument (Milford, MA) with a size exclusion column (Waters, BioSuite, 4 μm UHR SEC, 4.6 mm × 300 mm), employing isocratic chloroform/methanol/water/formic acid (400/400/90/25 v/v/v/v) flow at 0.25 mL min^{-1}, pH 2.5, 0 °C, and with 25 μL manual injections. The SEC column was coupled to the electrospray source of a Q-TOF Ultima API mass spectrometer (Waters).[69] Rapid side chain back exchange takes place during LC, such that only labeling information for backbone amides is retained.[34] Experimental spectra were converted to mass distributions using deconvolution software provided by the instrument manufacturer. Relative HDX levels of the intact protein were determined from the deconvoluted mass distributions using the relationship[36]

$$\text{deuteration percentage} = \frac{m - m_0}{m_{100} - m_0} \times 100\% \quad (3)$$

In this expression m is the measured mass (peak maximum) of the protein, and m_0 and m_{100} are the values of zero time point controls and maximally deuterated samples. Zero time point control data were obtained by exposing the protein first to the 0 °C quenching solution and then to the labeling buffer. Maximally deuterated protein samples were obtained by exposing refolded BO to labeling buffer for 24 h using the same conditions as for the light/dark samples. The uncorrected labeling level of these samples was 97% (229 out of 236 amide hydrogens), indicating the occurrence of 3% back exchange during analysis. Normalized HDX kinetics (eq 3) were analyzed by single- or double-exponential fitting using Sigmaplot. All data shown are based on triplicate independent experiments. Error bars correspond to standard deviations. Both proteolytic digestion[34] and top-down strategies[71,72] were pursued in an effort to obtain spatially resolved HDX information. Unfortunately, the sequence coverage of those experiments was not adequate, such that the considerations of this work must be restricted to HDX data at the intact protein level.

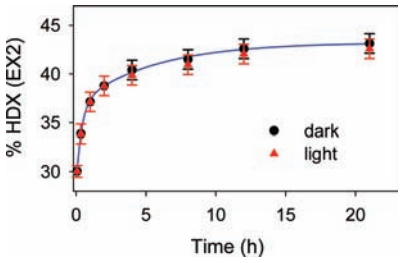

Figure 1. HDX kinetics of native BR in purple membranes monitored by ESI-MS. Red triangles and black circles represent data recorded under green light illumination (530 nm) and in the dark, respectively. The blue lines represent a biexponential fit, $D\%(t) = y_0 + a_1(1 - \exp[-k_1 t]) + a_2(1 - \exp[-k_2 t])$, with $y_0 = 28.7$, $a_1 = 8.1$, $k_1 = 2.56\ h^{-1}$, $a_2 = 6.4$, and $k_2 = 0.18\ h^{-1}$. Isotope exchange under the conditions of this experiment proceeds in the EX2 regime; no EX1-related peak splitting was observed in the BR mass distributions (not shown).

Flash Absorption Spectroscopy. Photocycle kinetics were measured by time-resolved difference spectroscopy, using a custom-built flash photolysis apparatus.[73] 0.5 mL of BR solution (prepared as above for HDX experiments) with an optical density of ~0.6 was placed in a cuvette, which allowed the 532 nm second harmonic of a Nd:YAG Minilite II laser to excite the sample at a 90° angle to the probe light beam from a Oriel QTH source. The photocycle was triggered with a 7 ns laser flash at room temperature. The resulting absorbance changes were recorded using a photomultiplier, amplifier, and Gage Compuscope AD converter. Up to 600 single-shot traces were averaged to produce an adequate signal-to-noise ratio.

RESULTS AND DISCUSSION

HDX Measurements on Purple Membranes. For comparing BR structural dynamics under illumination and in the dark by HDX-MS, investigations were initially conducted on intact purple membranes. Somewhat disappointingly, the isotope exchange behavior observed under light/dark conditions for these samples is virtually indistinguishable (Figure 1). Consistent with earlier reports,[69,74,75] purple membranes exhibit a high degree of protection. Even after an extended labeling period of 24 h, the BR deuteration level is only 43%. Although spatially resolved HDX studies on BR are difficult,[76] labeling under the conditions of Figure 1 is known to occur predominantly in peripheral regions, i.e., loops and helix termini.[55,69,74,77] Possible effects of light-induced CMs are expected to be most prevalent for transmembrane segments in the vicinity of the retinal.[55,57,58] Previous work[74] already implied that opening/closing events (eq 1) at these internal segments are exceedingly rare and/or short-lived, such that the lack of light-induced differences in Figure 1 is not completely surprising. Minor light-induced differences in exchange kinetics were reported in an older tritium exchange study.[78] However, those earlier purple membrane radiolabeling data[78] exhibited considerable scatter, and no error bars were reported. Under the conditions of our work, we cannot confirm the effects reported in ref 78. We do not dispute that purple membranes may undergo a certain "softening" upon illumination, as suggested by neutron scattering[26] and hydroxylaminolysis investigations.[66,79] Nonetheless, light-induced changes in structure and dynamics do not manifest themselves in altered HDX kinetics under the conditions of Figure 1.

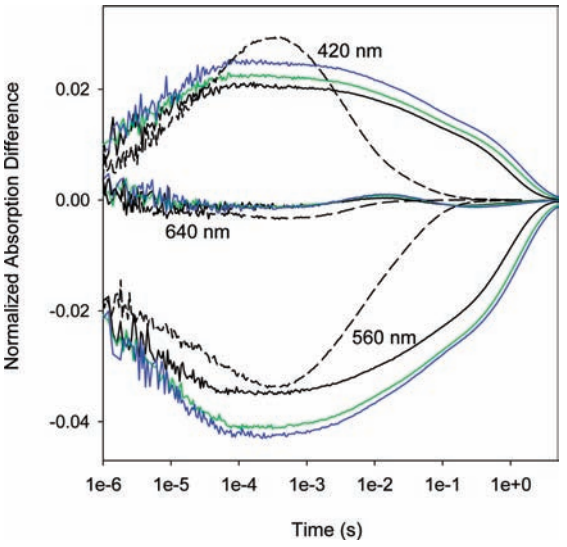

Figure 2. BR photocycle kinetics monitored by time-resolved absorption difference spectroscopy following a 532 nm excitation pulse. The transients were recorded at 560 nm (BR ground state), 420 nm (M intermediate), and 640 nm (O intermediate). Data are shown for monomeric BR without prior continuous illumination (black solid line), after 4 h of continuous illumination (green), and after 24 h of continuous illumination (blue). Also included are the kinetics of native purple membranes (black broken line). The data shown for each sample were normalized to the absorbance of the 568 nm retinal peak.

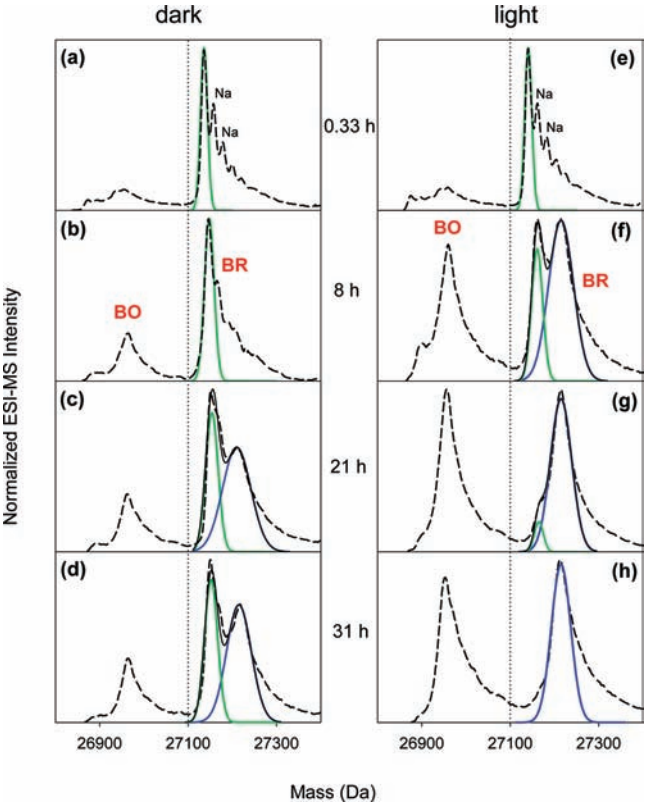

Figure 3. Mass distributions of monomeric BR at selected continuous-labeling HDX time points (0.33−31 h, as indicated in the figure). Panels a−d represent the behavior of samples that were kept in the dark. Data in panels e−h were recorded after continuous illumination of the protein. Black broken lines represent experimental spectra. Dotted vertical lines at 27100 Da separate contributions attributable to BO and BR, as highlighted in panels b and f. Gaussian curve fitting was employed to determine the locations of the peak areas and the maxima of BR. Green, EX2 component; blue, EX1 component; black solid line, sum of EX1 and EX2 components. The spectra show some sodium adduction (highlighted in parts a and e), which is a common occurrence in ESI-MS.

HDX Measurements on Monomeric BR. Packing effects inside the rigid 2D crystal lattice of the purple membrane[80] can restrict the extent of protein motions.[81,82] For the remainder of this study, we therefore shift our attention from purple membranes to monomeric BR in DMPC/CHAPS bicelles.[50] This form of the protein represents a well established model system that has been used in numerous earlier studies.[66,76,83,84] The monomeric form is known to undergo more extensive HDX,[69] reflecting greater overall dynamics with enhanced solvent access to formerly protected amide sites.[50]

Flash photolysis was used to verify that monomeric BR undergoes a photocycle (Figure 2, black solid lines).[28,85−87] The protein remains active even after extensive continuous illumination (Figure 2, green and blue lines), mimicking the conditions used for subsequent HDX experiments. For comparison, Figure 2 also shows data for intact purple membranes (black broken line) which reveal photocycle kinetics that are somewhat faster than those for the monomeric protein. The data of Figure 2 are consistent with earlier work on solubilized BR[88,89] where it was shown that reprotonation of the Schiff base is slower in the absence of the purple membrane lattice. These altered kinetics extend the lifetime of the M state and thus lead to a greater accumulation of this photocycle intermediate (as seen from the slower decay of the 420 nm signals in Figure 2). Overall, the data of Figure 2 confirm that monomeric BR is a functional molecular machine that continuously undergoes CMs upon illumination, albeit at a lower rate than that for purple membrane samples.

Monomeric BR displays HDX kinetics that are profoundly different in the dark (Figure 3a−d) and under illumination (Figure 3e−h). In both cases the protein exhibits a combination of EX2 and EX1 exchange. The former manifests itself as a gradual shift of the BR main peak to higher mass (highlighted in green, Figure 3). Superimposed on this EX2 process is the appearance of a highly deuterated EX1 component that increases in magnitude over time (Figure 3, blue). Combined EX1/EX2 processes have previously been observed for other proteins.[40,90,91]

Figure 3 also reveals the occurrence of BR → BO conversion, leading to ca. 50% retinal loss after 31 h of illumination (Figure 3h). This hydrolysis reaction can also be traced by UV−vis spectroscopy (data not shown). Retinal loss is less extensive in the dark (Figure 3d). The occurrence of retinal loss under illumination has previously been demonstrated for intact purple membranes, where the hydrolysis rate was shown to increase with pH.[92] Hence, the observation of this process under the conditions of the current work (monomeric BR at pH 8.5) is not unexpected. In Figure 2, this photodegradation is not apparent because the photocycle signals were normalized to the absorption maximum of the active protein. We emphasize that the MS approach used here allows the HDX kinetics of coexisting BR and BO to be monitored separately. As a result, the BR behavior can be probed without interference from BO signals (Figure 3). In other words, the BR data discussed below exclusively reflect the properties of the intact protein, prior to retinal loss.

Least-square analyses of the measured kinetics reiterate the considerable differences in HDX behavior for the light/dark

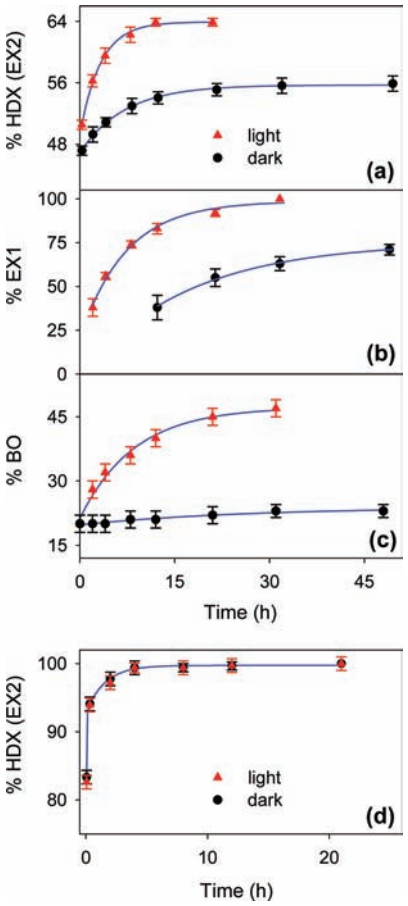

Figure 4. Kinetic behavior of monomeric BR under illumination (red) and in the dark (black). (a) EX2 HDX kinetics, determined from the maxima of the "green" component in Figure 3. (b) EX1 HDX kinetics, reflecting the rise of the "blue" component relative to the "green" one in Figure 3. (c) Percentage of BO in the protein samples as a function of time. Blue lines represent exponential fits with $y(t) = y_0 + a(1 - \exp[-kt])$. Fitting parameters: (a, light), $y_0 = 49$, $a = 15$, $k = 0.31\ h^{-1}$; (a, dark), $y_0 = 47$, $a = 9$, $k = 0.14\ h^{-1}$; (b, light), $y_0 = 20$, $a = 79$, $k = 0.14\ h^{-1}$; (b, dark), $y_0 \approx 0$, $a = 75$, $k = 0.06\ h^{-1}$; (c, light), $y_0 = 21$, $a = 26$, $k = 0.12\ h^{-1}$; (c, dark), $y_0 = 20$, $a = 4$, $k = 0.04\ h^{-1}$. These fitting parameters form the basis of the thermodynamic model which is presented below (Figure 5, Table 1). Panel d shows the results of control experiments, displaying a light/dark comparison of the EX2 HDX kinetics for pure BO samples (refolded in the absence of retinal).

samples. Illumination enhances the EX2 rate constant by a factor of 2 (Figure 4a; see caption for fitting parameters). A similar acceleration factor is seen for the EX1 process (Figure 4b). BO formation under illumination proceeds with an apparent rate constant of $0.12\ h^{-1}$. In the dark, this Schiff base hydrolysis is much slower, and the reaction rate cannot be readily determined (Figure 4c). The maximum of the EX1 component (blue peak envelopes in Figure 3) corresponds to an HDX level of 89% for all conditions studied. The BO peak maxima in Figure 3 reveal somewhat higher HDX levels, between 95% and 100%.

As noted in the Methods section, care was taken to ensure that comparative light/dark experiments were conducted in an artifact-free fashion. As an additional control, HDX studies were carried out on pure BO samples, i.e., monomeric protein that had been refolded in the absence of retinal. Figure 4d confirms that the HDX kinetics of these chromophore-free samples are indistinguishable under illumination and in the dark. This result reinforces the conclusion that the HDX differences seen for monomeric BR (Figures 3 and 4) are the result of light-induced protein structural dynamics.

Some readers might be tempted to ascribe the kinetic phenomena of Figure 3e–h *directly* to CMs that occur during the photocycle, possibly interpreting the EX1 "blue" peak as an accumulating photocycle intermediate. Unfortunately, such an interpretation is incorrect. The link between illumination and HDX behavior is more subtle, as can be seen from several arguments. First, the EX1 amide opening rate of $4 \times 10^{-5}\ s^{-1}$ (Figure 4b) is many orders of magnitude slower than the $\sim 1\ s^{-1}$ photocycle turnover rate (Figure 2). Thus, the EX1 peak cannot represent a photocycle intermediate. Also, X-ray crystallographic studies did not reveal any photocycle intermediates with a large number of open amide hydrogens[54] that would be required for HDX to proceed via eq 1. Most importantly, the general nature of the phenomena seen in Figure 3 (i.e., a combination of EX2 and EX1 with slow retinal loss) is the same in the dark and under illumination. Light exposure enhances the rates of these processes, while their overall character remains unchanged. It must be concluded that the protein motions that mediate HDX largely correspond to *intrinsic* TFs, rather than photocycle-associated CMs. The extent of these TFs is dramatically enhanced in the presence of light-induced CMs. Thus, TFs that mediate HDX are closely coupled to photon-driven CMs, but the two types of dynamics remain distinct from each other.

Casting the HDX Kinetics in a Thermodynamic/Kinetic Model. The data presented here allow the development of a minimalist model that can account for the HDX behavior of monomeric BR under light/dark conditions. Our considerations are based on eq 1, according to which HDX is mediated by TFs that result in amide hydrogen opening/closing transitions.[32] For reasons of simplicity, we assume that these fluctuations encompass distinct groups of amide hydrogens in a cooperative fashion. The interpretation of protein structural dynamics in terms of such cooperative units (foldons) is well established.[93,94]

For any protein, the occurrence of parallel EX1 and EX2 kinetics implies the involvement of at least four different conformational species.[40,91,95] EX2 exchange reflects rapid fluctuations between the natively folded state *F* and a native-like (but partially unfolded) excited species *F**. EX1 exchange can be attributed to the occurrence of infrequent transitions between *F* and a significantly unfolded conformer *U*. Slow interconversion between *F* and *U* requires crossing of a major free energy barrier that is associated with a transition state *TS*.[40,91,95] For clarity, we emphasize again that none of the four conformers *F*, *F**, *TS*, or *U* corresponds to a BR photocycle intermediate. Instead, the entire photocycle proceeds largely within the confines of the native conformational ensemble *F*. Thermally activated excursions to *F** or *U* are not directly linked to vectorial proton transport.

Figure 5 displays the number of open hydrogens for *F*, *F**, *TS*, and *U*, together with the corresponding free energy values. Light and dark scenarios are distinguished by subscripts. The free energy of *U* is arbitrarily normalized to zero. The number of open hydrogens in *U* is 89%, in accordance with the EX1 signals of Figure 3 (blue Gaussian curves). On the basis of its HDX level, *U* is extensively unfolded while retaining some residual protection. We make the simplifying assumption that the same transition state is encountered under illumination and in the dark. The positioning of all the species in the two-dimensional diagram of Figure 5 is consistent with the measured HDX parameters (Table 1). Only the location of the *TS* is somewhat arbitrary,

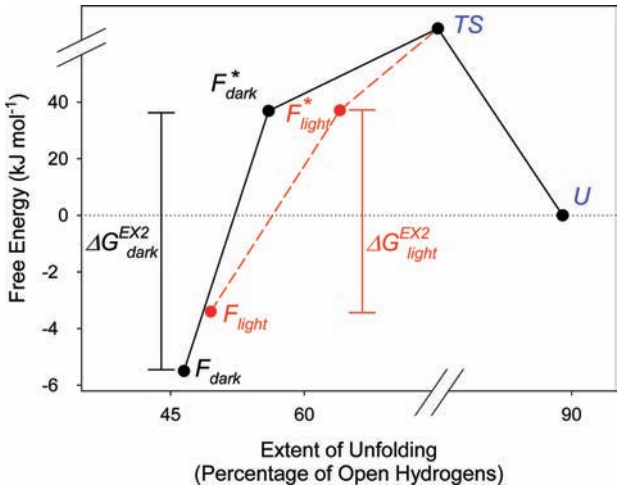

Figure 5. Schematic diagram, depicting thermodynamic and structural properties of monomeric BR conformers under illumination (red) and in the dark (black). Species highlighted in blue are common to both scenarios. The *x*-axis displays the percentage of amide hydrogens that adopt an open (unprotected) state. The *y*-axis represents free energy. The positioning of all species is consistent with the data displayed in Table 1. EX2 processes are mediated by fluctuations between *F* and *F**, whereas EX1 exchange arises due to interconversion between *F* and *U*. Note that the scaling of the free energy axis in this diagram is not linear, to emphasize differences between F_{dark} and F_{light}. Additional information is provided in the text.

Table 1. Structural and Thermodynamic Parameters Associated with the HDX Kinetics of Monomeric BR

	% open N−H sites in *F* [a]	ΔG^{EX2} (kJ mol^{-1}) [b]	% additional open N−H sites in *F** [c]	free energy difference between *U* and *F* (kJ mol^{-1})
light	49	40.5	15	3.4 [d]
dark	47	42.4	9	5.5 [e]

[a] EX2 burst phase amplitude (fitting parameter y_0) in Figure 4a. [b] Determined from eq 2, with $k_{ch} \approx 1000$ s^{-1}.[39,70] [c] EX2 amplitude (fitting parameter *a*) in Figure 4a. [d] Determined from the EX1 burst phase amplitude, which implies a [U]/[F] equilibrium ratio of 0.25 under illumination. [e] The ratio of the EX1 rates reflects an activation energy difference according to[22] $rate_1/rate_2 = \exp(\Delta\Delta G^{\#}/RT)$, where $|\Delta\Delta G^{\#}| = 2.1$ kJ mol^{-1}. In combination with footnote *d*, this implies an overall free energy difference of (3.4 + 2.1) kJ mol^{-1} = 5.5 kJ mol^{-1}.

since its properties cannot be ascertained with certainty from the data of this work.

Mechanistic Origin of Differences in Light/Dark HDX Behavior. The findings of this work reveal that illumination of monomeric BR causes subglobal as well as global destabilization of the protein. EX2 processes report on the former, whereas EX1 events are related to the latter. At the subglobal level, TFs involve a considerably larger number of EX2 sites under illumination (15%) than in the dark (9%, Table 1). This implies that transitions between *F* and *F** entail more extensive structural changes when the protein is exposed to light.[26] In other words, F^*_{light} represents a more unfolded conformation than F^*_{dark} (Figure 5). The occurrence of light-induced destabilization becomes most obvious when relating the ΔG^{EX2} values to the number of hydrogens involved. Accordingly, the average free energy required for the opening of a single EX2 site is 4.8 kJ mol^{-1} in the dark, but only 2.7 kJ mol^{-1} during illumination.

The EX1 behavior of monomeric BR suggests that illumination reduces the thermodynamic stability (i.e., the free energy difference between *F* and *U*) from 5.5 to 3.4 kJ mol^{-1} (Figure 5, Table 1). This destabilization causes *U* to be more highly populated in the light (∼ 20%) than in the dark (<10%).

In our view, Schiff base hydrolysis likely occurs from *U*. The Schiff base is sensitive to attack by water and other nucleophiles.[66,96] *U* represents a highly unfolded conformer that will not significantly protect the Schiff base from solvent access. A light-induced equilibrium shift from *F* to *U* will therefore lead to accelerated retinal loss, consistent with the behavior seen in Figure 4c.

CONCLUSIONS

HDX is mediated by opening/closing events of exchangeable hydrogens that occur as the result of TFs. In this work we examined the behavior of a molecular machine, with the goal of determining whether the extent of these TFs depends on the occurrence of CMs. BR is a molecular machine that is fueled by light. It is a simple matter to perform comparative measurements for this system under CM-on and CM-off conditions. Irrespective of the illumination state, monomeric BR undergoes two types of TFs. Small-scale EX2 fluctuations between the natively folded *F* and a native-like excited species *F** only affect a handful of N−H sites. In addition, *F* also undergoes rare EX1 transitions to a much more unfolded state *U*.

Amide hydrogen opening/closing events that are probed by HDX do *not* directly correspond to structural transitions between individual photocycle intermediates.[54,57−59] Yet, our experiments reveal dramatically enhanced HDX kinetics when the monomeric protein undergoes CMs in the presence of light. We attribute this phenomenon to a destabilizing effect of the light-driven *trans*/*cis* retinal switching cycle on the overall protein structure. The retinal is intimately coupled to the surrounding polypeptide elements.[97] Mechanical agitation of the chromophore is transferred to the protein scaffold, before the energy dissipates into the bulk solvent. The conversion of photon energy to mechanical motions is therefore comparable to the presence of a heat source in the protein interior. In other words, the enhanced TFs seen in our HDX experiments can be ascribed to local heating that occurs as the result of the protein's CMs. The heat involved in this phenomenon likely represents only a small fraction of the initially absorbed energy (226 kJ mol^{-1} for a 530 nm photon). Our interpretation of retinal movements as a source of thermal energy is consistent with earlier proposals.[92] We reiterate that the light/dark comparisons of this work were conducted at the same *bulk* temperature. On its way from the retinal "hot spot" to the thermostatted solvent, however, the thermal energy must pass through the protein, where it enhances TFs (opening/closing events) that promote HDX.

Investigations on various different systems have suggested that thermally activated conformational dynamics can "lubricate" certain aspects of protein function.[11,26,53,98] In this sense, it is to be expected that the light-enhanced TFs seen here for monomeric BR facilitate certain structural events that are associated with proton translocation. The absence of photoinduced HDX changes for intact purple membranes (Figure 1) appears to contradict this assertion. However, a likely explanation for the data of Figure 1 is the lack of solvent access,[69,74,75] which renders HDX insensitive to protein dynamics in the purple membrane

interior. In any case, the current study reveals that HDX-based TF measurements offer a window into the inner workings of molecular machines. In future work, it will be interesting to see if our findings can be corroborated for other proteins that have their function coupled to an external energy source.

■ ASSOCIATED CONTENT

Supporting Information. Complete ref 16 This material is available free of charge via the Internet at http://pubs.acs.org.

■ AUTHOR INFORMATION

Corresponding Author
konerman@uwo.ca

■ ACKNOWLEDGMENT

Funding for this work was provided by the Natural Sciences and Engineering Research Council of Canada (NSERC), the Canada Foundation for Innovation (CFI), and the Canada Research Chairs Program.

■ REFERENCES

(1) Liang, Z.-X.; Lee, T.; Resing, K. A.; Ahn, N. G.; Klinman, J. P. *Proc. Natl. Acad. Sci. U.S.A.* **2004**, *101*, 9556–9561.
(2) Codreanu, S. G.; Ladner, J. E.; Xiao, G.; Stourman, N. V.; Hachey, D. L.; Gilliland, G. L.; Armstrong, R. N. *Biochemistry* **2002**, *41*, 15161–15172.
(3) Wolf-Watz, M.; Thai, V.; Henzler-Wildman, K.; Hadjipavlou, G.; Eisenmesser, E. Z.; Kern, D. *Nat. Struct. Mol. Biol.* **2004**, *11*, 945–949.
(4) Hollien, J.; Marqusee, S. *Proc. Natl. Acad. Sci. U.S.A.* **1999**, *96*, 13674–13678.
(5) Pagán, M.; Solá, R. J.; Griebenow, K. *Biotechnol. Bioeng.* **2008**, *103*, 77–83.
(6) Zavodszky, P.; Kardos, J.; Svingor, A.; Petsko, A. G. *Proc. Natl. Acad. Sci.* **1998**, *95*, 7406–7411.
(7) Bhabha, G.; Lee, J.; Ekiert, D. C.; Gam, J.; Wilson, I. A.; Dyson, H. J.; Benkovic, S. J.; Wright, P. E. *Science* **2011**, *332*, 234–238.
(8) Schwartz, S. D.; Schramm, V. L. *Nat. Chem. Biol.* **2009**, *5*, 551–558.
(9) Pisliakov, A. V.; Cao, J.; Kamerlin, S. C. L.; Warshel, A. *Proc. Natl. Acad. Sci. U.S.A.* **2009**, *106*, 17359–17364.
(10) Kamerlin, S. C. L.; Warshel, A. *Proc. Natl. Acad. Sci. U.S.A.* **2010**, *107*, E72.
(11) Karplus, M. *Proc. Natl. Acad. Sci. U.S.A.* **2010**, *107*, E71.
(12) Henzler-Wildman, K.; Kern, D. *Nature* **2007**, *450*, 964–972.
(13) Boehr, D. D.; Nussinov, R.; Wright, P. E. *Nat. Chem. Biol.* **2009**, *5*, 789–796.
(14) Diallinas, G. *Science* **2008**, *322*, 1644–1645.
(15) Singh, S. K.; Piscitelli, C. L.; Yamashita, A.; Gouaux, E. *Science* **2008**, *322*, 1655–1661.
(16) Weyand, S.; et al. *Science* **2008**, *322*, 709–713.
(17) Diez, M.; Zimmermann, B.; Börsch, M.; König, M.; Schweinberger, E.; Steigmiller, S.; Reuter, R.; Felekyan, S.; Kudryavtsev, V.; Seidel, C. A.; Gräber, P. *Nat. Struct. Mol. Biol.* **2004**, *11*, 135–141.
(18) Gennerich, A.; Vale, R. D. *Curr. Opin. Cell Biol.* **2009**, *21*, 59–67.
(19) Frauenfelder, H.; Chen, G.; Berendzen, J.; Fenimore, P. W.; Jansson, H.; McMahon, B. H.; Stroe, I. R.; Swenson, J.; Young, R. D. *Proc. Natl. Acad. Sci. U.S.A.* **2009**, *106*, 5129–5134.
(20) Ansari, A.; Berendzen, J.; Bowne, S. F.; Frauenfelder, H.; Iben, I. T.; Sauke, T. B.; Shyamsunder, E.; Young, R. D. *Proc. Natl. Acad. Sci. U.S.A.* **1985**, *82*, 5000–5004.
(21) Bai, Y.; Sosnick, T. R.; Mayne, L.; Englander, S. W. *Science* **1995**, *269*, 192–197.
(22) Bieri, O.; Kiefhaber, T. In *Mechanisms of Protein Folding*; Pain, R. H., Ed.; University Press: Oxford, 2000.
(23) Liu, Y.; Belcheva, A.; Konermann, L.; Golemi-Kotra, D. *J. Mol. Biol.* **2009**, *391*, 149–163.
(24) Sugase, K.; Dyson, H. J.; Wright, P. E. *Nature* **2007**, *447*, 1021–1027.
(25) Pieper, J.; Renger, G. *Biochemistry* **2009**, *48*, 6111–6115.
(26) Pieper, J.; Buchsteiner, A.; Dencher, N. A.; Lechner, R. E.; Hauß, T. *Phys. Rev. Lett.* **2008**, *100*, 2281031–2281034.
(27) Langosch, D.; Arkin, I. T. *Protein Sci.* **2009**, *18*, 1343–1358.
(28) Simón-Vázquez, R.; Lazarova, T.; Perálvarez-Marín, A.; Bourdelande, J. L.; Padrós, E. *Angew. Chem., Int. Ed.* **2009**, *48*, 8523–8525.
(29) Shaw, D. E.; Maragakis, P.; Lindorff-Larsen, K.; Piana, S.; Dror, R. O.; Eastwood, M. P.; Bank, J. A.; Jumper, J. M.; Salmon, J. K.; Shan, Y.; Wriggers, W. *Science* **2010**, *330*, 341–346.
(30) Rhoades, E.; Cohen, M.; Schuler, B.; Haran, G. *J. Am. Chem. Soc.* **2004**, *126*, 14686–14687.
(31) Mittermaier, A.; Kay, L. E. *Science* **2006**, *312*, 224–228.
(32) Krishna, M. M. G.; Hoang, L.; Lin, Y.; Englander, S. W. *Methods* **2004**, *34*, 51–64.
(33) Kaltashov, I. A.; Eyles, S. J. *Mass Spectrometry in Biophysics*; John Wiley and Sons, Inc.: Hoboken, NJ, 2005.
(34) Houde, D.; Berkowitz, S. A.; Engen, J. R. *J. Pharm. Sci.* **2011**, *100*, 2071–2086.
(35) Miranker, A.; Robinson, C. V.; Radford, S. E.; Aplin, R.; Dobson, C. M. *Science* **1993**, *262*, 896–900.
(36) Smith, D. L.; Deng, Y.; Zhang, Z. *J. Mass Spectrom.* **1997**, *32*, 135–146.
(37) Hvidt, A.; Nielsen, S. O. *Adv. Protein Chem.* **1966**, *21*, 287–386.
(38) Chetty, P. S.; Mayne, L.; Lund-Katz, S.; Stranz, D. D.; Englander, S. W.; Phillips, M. C. *Proc. Natl. Acad. Sci. U.S.A.* **2009**, *106*, 19005–19010.
(39) Bai, Y.; Milne, J. S.; Mayne, L.; Englander, S. W. *Proteins: Struct. Funct. Genet.* **1993**, *17*, 75–86.
(40) Konermann, L.; Tong, X.; Pan, Y. *J. Mass Spectrom.* **2008**, *43*, 1021–1036.
(41) Johnson, R. S.; Walsh, K. A. *Protein Sci.* **1994**, *3*, 2411–2418.
(42) Englander, J. J.; Del Mar, C.; Li, W.; Englander, S. W.; Kim, J. S.; Stranz, D. D.; Hamuro, Y.; Woods, V. L. *Proc. Natl. Acad. Sci. U.S.A.* **2003**, *100*, 7057–7062.
(43) Xiao, H.; Kaltashov, I. A.; Eyles, S. J. *J. Am. Soc. Mass Spectrom.* **2003**, *14*, 506–515.
(44) Busenlehner, L. S.; Salomonsson, L.; Brzezinski, P.; Armstrong, R. N. *Proc. Natl. Acad. Sci. U.S.A.* **2006**, *103*, 15398–15403.
(45) Sperry, J. B.; Smith, C. L.; Caparon, M. G.; Ellenberger, T.; Gross, M. L. *Biochemistry* **2011**, *50*, 4038–4045.
(46) Chalmers, M. J.; Busby, S. A.; Pascal, B. D.; He, Y.; Hendrickson, C. L.; Marshall, A. G.; Griffin, P. R. *Anal. Chem.* **2006**, *78*, 1005–1014.
(47) Marcoux, J.; Manb, P.; Castellan, M.; Vives, C.; Forest, E.; Fieschi, F. *FEBS Lett.* **2009**, *583*, 835–840.
(48) Powell, K. D.; Ghaemmaghami, S.; Wang, M. Z.; Ma, L.; Oas, T. G.; Fitzgerald, M. C. *J. Am. Chem. Soc.* **2002**, *124*, 10256–10257.
(49) Dencher, N. A.; Sass, H. J.; Büldt, G. *Biochim. Biophys. Acta* **2000**, *1460*, 192–203.
(50) Brouillette, C. G.; Mcmichens, R. B.; Stern, L. J.; Khorana, H. G. *Proteins: Struct. Funct. Genet.* **1989**, *5*, 38–46.
(51) Subramaniam, S.; Hirai, T.; Henderson, R. *Philos. Trans. R. Soc. London, A* **2002**, *360*, 859–874.
(52) Haupts, U.; Tittor, J.; Oesterhelt, D. *Annu. Rev. Biophys. Biomol. Struct.* **1999**, *28*, 367–399.
(53) Heberle, J.; Fitter, J.; Sass, H. J.; Büldt, G. *Biophys. Chem.* **2000**, *85*, 229–248.
(54) Lanyi, J. K. *Annu. Rev. Physiol.* **2004**, *66*, 665–688.
(55) Kluge, T.; Olejnik, J.; Smilowitz, L.; Rothschild, K. J. *Biochemistry* **1998**, *37*, 10279–10285.
(56) Shibata, M.; Yamashita, H.; Uchihashi, T.; Kandori, K.; Ando, T. *Nat. Nanotechnol.* **2010**, *5*, 208–212.

(57) Luecke, H.; Schobert, B.; Richter, H. T.; Cartailler, J. P.; Lanyi, J. K. *Science* **1999**, *286*, 255–261.
(58) Sass, H. J.; Büldt, G.; Gessenich, R.; Hehn, D.; Neff, D.; Schlesinger, R.; Berendzen, J.; Ormos, P. *Nature* **2000**, *406*, 649–653.
(59) Hirai, T.; Subramaniam, S. *PLoS One* **2009**, *4*, e5769.
(60) Andersson, M.; Malmerberg, E.; Westenhoff, S.; Katona, G.; Cammarata, M.; Wö hri, M. B.; Johansson, L. C.; Ewald, F.; Eklund, M.; Wulff, M.; Davidsson, J.; Neutze, R. *Structure* **2009**, *17*, 1265–1275.
(61) Patzelt, H.; Simon, B.; terLaak, A.; Kessler, B.; Kühne, R.; Schmieder, P.; Oesterhelt, D.; Oschkinat, H. *Proc. Natl. Acad. Sci. U.S.A.* **2002**, *99*, 9765–9770.
(62) Nishikawa, T.; Murakami, M.; Kouyama, T. *J. Mol. Biol.* **2005**, *352*, 319–328.
(63) Ni, B.; Chang, M.; Duschl, A.; Lanyi, J.; Needleman, R. *Gene* **1990**, *90*, 169–172.
(64) Pan, Y.; Stocks, B. B.; Brown, L.; Konermann, L. *Anal. Chem.* **2009**, *81*, 28–35.
(65) Oesterhelt, D.; Stoeckenius, W. *Methods Enzymol.* **1974**, *31*, 667–678.
(66) Subramaniam, S.; Marti, T.; Rösselet, S. J.; Rothschild, K. J.; Khorana, H. G. *Proc. Natl. Acad. Sci. U.S.A.* **1991**, *88*, 2581–2587.
(67) Pan, Y.; Brown, L.; Konermann, L. *J. Mol. Biol.* **2011**, *410*, 146–158.
(68) Booth, P. J.; Farooq, A.; Flitsch, S. L. *Biochemistry* **1996**, *35*, 5902–5909.
(69) Pan, Y.; Brown, L.; Konermann, L. *Int. J. Mass Spectrom.* **2011**, *302*, 3–11.
(70) Roder, H.; Elöve, G. A.; Englander, S. W. *Nature* **1988**, *335*, 700–704.
(71) Sterling, H. J.; Williams, E. R. *Anal. Chem.* **2010**, *82*, 9050–9057.
(72) Pan, J.; Han, J.; Borchers, C. H.; Konermann, L. *J. Am. Chem. Soc.* **2009**, *131*, 12801–12808.
(73) Waschuk, S. A.; Bezerra, A. G.; Shi, L.; Brown, L. S. *Proc. Natl. Acad. Sci. U.S.A.* **2005**, *102*, 6879–6883.
(74) Englander, J. J.; Englander, S. W. *Nature* **1977**, *265*, 658–659.
(75) Downer, N. W.; Bruchman, T. J.; Hazzard, J. H. *J. Biol. Chem.* **1986**, *261*, 3640–3647.
(76) Joh, N. H.; Min, A.; Faham, S.; Whitelegge, J. P.; Yang, D.; Woods, V. L.; Bowie, J. U. *Nature* **2008**, *453*, 1266–1270.
(77) Earnest, T. N.; Herzfeld, J.; Rothschild, K. J. *Biophys. J.* **1990**, *58*, 1539–1546.
(78) Konishi, T.; Packer, L. *FEBS Lett.* **1977**, *80*, 455–458.
(79) Oesterhelt, D.; Schuhmann, L.; Gruber, H. *FEBS Lett.* **1974**, *44*, 257–261.
(80) Henderson, R.; Unwin, P. N. *Nature* **1975**, *257*, 28–32.
(81) Hirai, T.; Subramaniam, S.; Lanyi, J. K. *Curr. Opin. Struct. Biol.* **2009**, *19*, 433–439.
(82) Varo, G.; Lanyi, J. K. *Biochemistry* **1991**, *30*, 7165–7171.
(83) Curnow, P.; Booth, P. J. *Proc. Natl. Acad. Sci. U.S.A.* **2009**, *106*, 773–778.
(84) Curnow, P.; Di Bartolo, N. D.; Moreton, K. M.; Ajoje, O. O.; Saggese, N. P.; Booth, P. J. *Proc. Natl. Acad. Sci. U.S.A.* **2011**, *108*, 14133–14138.
(85) Balashov, S. P.; Lu, M.; Imasheva, E. S.; Govindjee, R.; Ebrey, T. G.; Othersen, B., III; Chen, Y.; Crouch, R. K.; Menick, D. R. *Biochemistry* **1999**, *38*, 2026–2039.
(86) Ludmann, K.; Gergely, C.; Váró, G. *Biophys. J.* **1998**, *75*, 3110–3119.
(87) Chizhov, I.; Engelhard, M.; Chernavskii, D. S.; Zubov, B.; Hess, B. *Biophys. J.* **1992**, *61*, 1001–1006.
(88) Marti, T.; Otto, H.; Mogi, T.; Rösselet, S. J.; Heyn, M. P.; Khorana, H. G. *J. Biol. Chem.* **1991**, *266*, 6919–6927.
(89) Váró, G.; Lanyi, J. *Biochemistry* **1991**, *30*, 5008–5015.
(90) Kim, M.-Y.; Maier, C. S.; Reed, D. J.; Deinzer, M. L. *Protein Sci.* **2002**, *11*, 1320–1329.
(91) Miranker, A.; Robinson, C. V.; Radford, S. E.; Dobson, C. M. *FASEB J.* **1996**, *10*, 93–101.
(92) Dancsházy, Z.; Tokaji, Z.; Dér, A. *FEBS Lett.* **1999**, *450*, 154–157.
(93) Maity, H.; Maity, M.; Krishna, M. M. G.; Mayne, L.; Englander, S. W. *Proc. Natl. Acad. Sci. U.S.A.* **2005**, *102*, 4741–4746.
(94) Weinkam, P.; Zimmermann, J.; Romesberg, F. E.; Wolynes, P. G. *Acc. Chem. Res.* **2010**, *43*, 652–660.
(95) Xiao, H.; Hoerner, J. K.; Eyles, S. J.; Dobo, A.; Voigtman, E.; Melcuk, A. I.; Kaltashov, I. A. *Protein Sci.* **2005**, *14*, 543–557.
(96) Jastrzebska, B.; Palczewski, K.; Golczak, M. *J. Biol. Chem.* **2011**, *286*, 18930–18937.
(97) Curnow, P.; Booth, P. J. *J. Mol. Biol.* **2010**, *403*, 630–642.
(98) Döring, K.; Surrey, T.; Grunewald, S.; John, E.; Jähnig, F. *Protein Sci.* **2000**, *9*, 2246–2250.